ULTRAWIDEFIELD AUTOFLUORESENCE IN ABCA4 STARGARDT DISEASE

MICHAEL A. KLUFAS, MD,* IRENA TSUI, MD,*† SRINIVAS R. SADDA, MD,† HAMID HOSSEINI, MD,* STEVEN D. SCHWARTZ, MD*

Purpose: To report the ultrawidefield fundus autofluorescence (UWF-FAF) patterns in ABC4A Stargardt disease.

Methods: A retrospective cohort study of patients with a clinical diagnosis of Stargardt disease, confirmed ABCA4 genotype, and ultrawidefield fundus autofluorescence imaging using an Optos P200Tx. Four independent graders evaluated the images. Ultrawidefield fundus autofluorescence images were evaluated for the presence of posterior pole and peripheral findings, and were classified into one of three types (Type I: lesions confined to the macula with no peripheral findings; Type II: macular atrophy with flecks only in the periphery; Type III: macular atrophy and varying degrees of peripheral atrophy).

Results: Ultrawidefield fundus autofluorescence was performed on 58 eyes of 29 patients. Reviews of images revealed the presence of peripheral (outside the 55° view of standard nonwidefield FAF imaging) alterations on UWF-FAF in 76% of eyes. Overall, the UWF-FAF pattern was classified as Type I in 24% eyes (14/58), Type II in 24% (14/58), and Type III in 52% (30/58). The most common genetic mutations were c.2588G>C (6/29 patients, 20.7%), and c.5882G>A (5/29 patients, 17.2%).

Conclusion: Ultrawidefield fundus autofluorescence reveals peripheral changes in the majority of patients with Stargardt disease. Peripheral FAF changes may have implications for diagnosis, prognosis, and management of individual patients with Stargardt disease.

RETINA 0:1–13, 2017

As is true in many conditions, the definition of Stargardt disease (STGD) has substantially narrowed since first described by Stargardt in 1909.[1] Despite this refinement, STGD remains the most common juvenile macular dystrophy with an incidence of ~1/10,000 individuals worldwide.[2] Clinically, patients typically present with central vision loss in childhood or early adulthood, central scotomata, and irregular yellow-white outer retinal flecks, and an atrophic maculopathy which may be progressive throughout life.[3] Significant clinical heterogeneity exists in the findings, presentation, severity, and course of STGD phenotypes among families with the disorder, even in patients with similar genotypes.[4–8] Furthermore, even though presenting changes often occur in the macula, and early definitions focus on macular features of the condition, numerous reports indicate there is widespread retinal dysfunction as evidenced by clinical examination, visual field testing,[9] and electroretinography.[10]

The majority of STGD cases are caused by autosomal recessive mutations of ABCA4,[11] but Stargardt-like phenotypes may be inherited in an autosomal dominant manner with mutations in PROM1[12] and ELOVL4.[13] Mutations in ABCA4 may also cause related disorders such as cone-rod dystrophy and autosomal recessive retinitis pigmentosa,[14] or potentially age-related macular degeneration.[15] ABC4A encodes an adenosine triphosphate (ATP)-binding cassette (ABC) transport protein expressed in both cones and rods, which is involved in the transport of all-*trans*-retinal. As a critical substrate in the visual cycle, perturbation of the transport of all-*trans*-retinal negatively impacts this complex cascade of cellular, enzymatic, and biochemical processes. Once outer segment shedding and subsequent phagocytosis of the outer segment by the retinal pigment epithelium

From the *Stein Eye Institute, University of California, Los Angeles, California; and †Doheny Eye Institute, University of California, Los Angeles, California.

Stein Eye Institute receives an unrestricted departmental grant from the Research to Present Blindness (RPB) foundation. M. A. Klufas was supported for a vitreoretinal surgery fellowship as a John and Theiline McCone Fellow at the Stein Eye Institute, University of California, Los Angeles.

Presented at the American Academy of Ophthalmology Annual Meeting, October 17th, 2016 Chicago, Illinois.

S. R. Sadda is a consultant for Optos, PLC. The remaining authors have no conflicting interests to disclose.

Reprint requests: Michael A. Klufas, MD, 100 Stein Plaza, Los Angeles, CA 90095; e-mail: mklufas@gmail.com

(RPE) occurs, all-*trans*-retinal is converted to a bisretinoid, A2E (N-retinylidene-N-retinylethanolamine), and then further processed by the visual cycle. A2E, which has been thought to be a major component of lipofuscin, accumulates with the abnormal ABC transport protein, and leads to the death of the RPE cells and overlying photoreceptors.[16]

Over 800 mutations in the *ABCA4* gene may cause autosomal recessive STGD with a wide range of effects on ABCR protein function.[17] Phenotypes of this disorder exhibit tremendous variability because of extensive genetic heterogeneity,[18,19] nonexomic mutations,[20] high carrier frequency of pathogenic ABC4A alleles in the general population (~1/20), and clinical variability with the general course of the disease (i.e., unique phenotype at a specific time point). Given the significant allelic heterogeneity, the relative pathogenic contribution of individual alleles remains difficult to assess since few individuals share the same biallelic combinations.[21] The combinations of mutations within a particular individual suggest the phenotype may be predicted by the functionality of the remaining ABCA4 protein, with lower amounts of functional protein being associated with more severe disease.[22] It has also been suggested that certain types of mutations such as truncating, severe misfolding, and intronic or splice-variant mutations may result in increased functional loss of ABCR protein and more severe disease.[23] Phenotypic evaluation might be greatly enhanced by reproducibly assessing general RPE function, specifically assessing the visual cycle through the presence and absence of photoreceptor outer segment metabolites.

Fundus autofluoresence (FAF) is a noninvasive imaging modality[24] that has increased in popularity with modern confocal scanning laser ophthalmoscope systems.[25] It can readily identify areas of atrophy with decreased autofluoresence associated with RPE cell death as well as accumulation of lipofuscin with areas of increased hyperautofluorescent signal in STGD.[26] Reports have indicated the utility of FAF to follow STGD disease progression over time, as the autoflourescent signal indicates the relative state of the visual cycle.[27,28] Fundus autofluoresence using a 30 to 55 degree imaging, has led to a description of 3 types of FAF patterns in the posterior pole in STGD.[29] A previous report has attempted to correlate nonwidefield FAF to genotypes in STGD.[30] Widefield FAF has been used to expand upon the description and classification of other retinal dystrophies,[31,32] age-related macular degeneration,[33] and retinal detachment.[34] The purpose of the current study is to report ultrawidefield fundus autofluorescence (UWF-FAF) imaging characteristics and patterns in ABC4A STGD.

Methods

A retrospective review was conducted at the Stein Eye Institute, University of California, Los Angeles, of patients examined between 2012 and 2016 with Institutional Review Board approval. Patients with positive ABCA4 genotyping and ophthalmoscopic findings consistent with Stargardt macular dystrophy (white-yellow flecks at the level of the RPE, RPE changes, macular atrophy/bull's eye macular atrophy), and were considered eligible for the study. Only patients who also had had Optos UWF-FAF performed were included.

A review of electronic medical records was performed in which demographic data, medical history, ocular history, visual acuity, slit lamp biomicroscopy, ophthalmoscopy, and other ancillary testing including fundus photography, optical coherence tomography, fluorescein angiography, electrooculography, and electroretinography (ERG) were reviewed when available.

Ultrawidefield fundus autofluorescence was obtained using a 532 nm excitation and 570 nm to 580 nm detection strategy with the Optos 200Tx scanning laser ophthalmoscope (Optos PLC, Dunfermline, Scotland, United Kingdom). Although the camera is able to capture images without dilation, patients were routinely dilated for clinical examination at the same visit. The images from both eyes of each patient were chosen for descriptive image analysis.

Images were evaluated for patterns of abnormal autofluoresence: macular atrophy (fovea sparing vs. not fovea sparing), hyperfluorescent flecks (macular vs. peripheral), hypofluorescent flecks (macular vs. peripheral), as well as other abnormalities, with particular attention to the transition zone between the peripheral-most extent of the flecks and normal appearing anterior retina. The presence or absence of peripapillary sparing was also noted. To compare images obtained from the Optos UWF-FAF with traditional FAF, an outline of this typical 55° field was superimposed on the Optos image using Photoshop CS5 software (Photoshop CS5; Adobe, San Jose, CA). Four experienced trained readers (S.D.S., V.S., I.T., M.A.K.) independently analyzed each UWF-FAF image for the presence of retinal pathology. Special attention was paid to the peripheral retina, defined as the region outside the 55° field of view which can be achieved with traditional FAF platforms.

A previous study described FAF pattern subtypes in STGD, but used nonwidefield imaging describing patterns confined to the posterior pole (30–55°).[29] A new UWF-FAF classification is described and implemented in this study with three patterns: Type I, Type II, and Type III (Table 1). Briefly, Type I consisted of lesions confined to the macula with no

Table 1. UWF-FAF Patterns in Stargardt disease

Classification with UWF-FAF		
Type I	Central atrophy with or without flecks confined to posterior pole—*No findings outside 55° field of view*	
Type II	Central atrophy with *flecks only* extending outside posterior pole	
Type III	Central atrophy and significant extramacular *flecks and atrophy* extending outside posterior pole	Subtypes A: mild/moderate atrophy (most often in punctate pattern) extending to or beyond equator B: severe atrophy extending from macula to equator C: extensive, severe atrophy extending anterior to equator

Posterior pole defined as 55° field of view found in standard non-widefield FAF systems.

peripheral findings. Type II consisted of macular atrophy with FAF alterations corresponding to flecks in the periphery. Type III consisted of macular and peripheral atrophy with three subtypes of peripheral atrophy patterns defined: IIIA—mild to moderate atrophy (most often in a punctate pattern) extending to or beyond the equator; IIIB—severe atrophy extending from macula to equator; IIIC—extensive, severe atrophy extending anterior to the equator (Table 1).

Descriptive statistics were performed in Microsoft Excel (Microsoft Inc, Redmond, WA). A one-way analysis of variance was performed to evaluate the effect of age on UWF-FAF subtype using SPSS Version 24 (SPSS Inc, Chicago, IL).

Genetic testing was performed by Prevention Genetics (Marshfield, WI), Casey Eye Institute Molecular Diagnostic Laboratory (Portland, OR), EyeGene (NIH, Bethesda, MD), or GeneDx (Gaithersburg, MD). Standard PCR amplification and sequencing of full coding regions for each patient were performed and compared with reference standards. All differences and sequence variants were reported.

Results

Twenty-nine patients were included in this study; 66.5% (N = 19) of patients were women. The average age was 46 years (range 22–73 years, SD 15 years); 46.4% (N = 13 patients) were younger than 45 years of age. Visual acuity at time of imaging, as well as other demographic data and summary of the cohort, are presented in Table 2.

Ultrawidefield fundus autofluorescence classification, UWF-FAF characteristics, and corresponding genotype for each patient are shown in Table 2. Of note, the assigned UWF-FAF classification was the same in both eyes of all subjects in this cohort, yielding a congruent classification in 100% of patients (29/29). About other characteristics of the lesions, such as the presence of peripapillary or foveal sparing, findings were symmetric in 89.6% of cases (26/29, 2 cases with asymmetric foveal sparing, 1 case of asymmetric peripapillary sparing). Overall, the UWF-FAF pattern was classified as Type I (Figure 1) in 24% eyes (14/58), Type II (Figure 2) in 24% (14/58), and Type III in 52% (30/58). The eyes deemed to be Type III were further subclassified based on the pattern of peripheral atrophy, and 13.7% of eyes were Type IIIa (Figure 3), 20.1% Type IIIb (Figure 4), 6.9% Type IIIa/IIIb (Figure 5), and 10.3% Type IIIc (Figure 6). Among the 13 patients less than 45 years of age at the time of UWF-FAF imaging, 38.5% (5/13) had Type III classification, 38.5% (5/13) had Type I classification, and 23.1% (3/13) had Type II classification. A one-way analysis of variance between subjects was conducted to compare the effect of patient age on UWF-FAF Type (I/II/III), and was not found to be statistically significant [$F_{(2,26)} = 1.397$, $P = 0.265$]. Similarly, a one-way analysis of variance to evaluate the effect of age on all UWF-FAF subtypes (I/II/IIIa/IIIb/IIIc) was performed, also yielding a nonstatistically significant result [$F_{(4,24)} = 0.664$, $P = 0.623$]. Therefore, patient age does not appear to be associated with UWF-FAF type in this cohort.

Additional peripheral UWF-FAF (outside 55°) abnormalities were also noted in 72.4% of cases (21/29). Peripheral increased hyperautofluoresence at the anterior border of the peripheral flecks at the presumed transition zone to a "normal-appearing" (or at least, less diseased) retina was noted in 41.4% of eyes (24/58, Figure 7). A posterior polar zone of increased hyperautofluoresence in a circular pattern outside the arcades was observed in 24.1% of eyes (14/58, Figure 8). Other infrequent peripheral findings on UWF-FAF images included: 1) one case (Type II classification) with a temporal semicircular crescent moon-shaped patch of increased hyperautofluoresence in both eyes anterior to the FAF abnormalities corresponding to peripheral flecks, and 2) an additional case with mottled peripheral FAF with areas of increased and

Table 2. Summary of Cohort

UWF-FAF Type	ID	Age	Sex	VA OD	VA OS	Gene 1	Gene 2	Gene 3
I	4	23	F	20/60	20/60	c.564delA	c.2588G>C	N/A
I	9	39	F	20/500	20/320	c.1804C>T	c.5882G>A	c.6729 +21C>T
I	10	23	M	20/70	20/80	c.1995C>A	c.5882G>A	c.4256T>C
I	12	42	F	20/250	20/250	c.2829delG	c.5882G>A	N/A
I	13	28	F	20/250	20/200	c.5882G>A	c.5917delG	N/A
I	17	54	M	20/40	20/100	c.1622T>C	c.3113C>T	N/A
I	29	53	F	CF 2FT	CF 3FT	c.4771G>A	none	N/A
II	1	50	F	20/200	20/200	c.2588G>C	c.4139C>T	N/A
II	2	62	M	20/125	20/250	c.5461-10T>C	N/A	N/A
II	5	53	F	20/160	20/100	c.2588G>C	c.4918C>T	c.2828 G>A
II	8	45	F	CF 8FT	20/200	c.2041C>T	c.6089G>A	N/A
II	11	73	M	20/800	20/800	c.5882G>A	none	N/A
II	15	37	M	20/300	CF 2FT	c.5714+5G>A	c.5898+2T>C	N/A
II	16	22	M	20/125	20/100	c.1622T>C	c.5714+5G>A	c.3113C>T
IIIa	3	59	F	CF 3FT	CF 3FT	c.2588G>C	c.5461-10T>C	N/A
IIIa	6	32	F	20/150	20/100	c.1715G>A	c2588G>C	c.5206T>C
IIIa	19	36	F	20/150	20/250	c.4537dupC	c.6686T>C	N/A
IIIa	24	58	M	20/250	20/250	c.71G>A	c.4222T>C and c.4918C>T	N/A
IIIa/IIIIb	14	46	M	HM	HM	c.5917delG	c.1018T>C	N/A
IIIa/IIIb	27	25	F	HM	HM	c.5318C>T	c.5318C>T	N/A
IIIb	7	65	M	CF 2FT	CF 2FT	c.2041C>T	c.2588G>C	N/A
IIIb	18	51	F	20/40	20/60	c.4519G>A	c.6221G>T	N/A
IIIb	22	53	F	HM	HM	c.768G>T	c.3304G>T	N/A
IIIb	23	68	F	20/400	20/300	c.71G>A	c.4222T>C and c.4918C>T	N/A
IIIb	26	54	M	HM	CF	IVS12+2T>G	IVS12+2T>G	N/A
IIIb	28	28	F	CF 1FT	CF 1FT	c.1619_1622delCTCT	c.5196+1G>A	N/A
IIIc	20	25	F	20/400	20/500	c.4577C>T	c.2161-8G>A	N/A
IIIc	21	57	F	CF 2FT	CF FACE	c.4469 G>A	none	N/A
IIIc	25	63	F	CF 1FT	20/100	c.4594G>A	c.4222T>C and c.4918C>T	N/A

UWF-FAF Type	ID	Peripapillary Sparing (Y/N)	Fovea Sparing (Y/N)	OS Same? (Y/N)	Other UWF- FAF Findings	ERG Results
I	4	Y	Y	Y	none	slightly decreased cone and rod function
I	9	Y	Y	Y	none	normal, no cone dystrophy
I	10	Y	Y	Y	posterior pole hypeFAF OU	mildly reduced cones
I	12	Y	Y	Y	posterior pole hypeFAF OU	none
I	13	Y	N	Y	posterior pole hypeFAF OU	dark adapted responses normal, condition may be limited to macula
I	17	Y	Y	Y—temporal hypoFAF from laser scars to HST	posterior pole hypeFAF OU	borderline abnormal under photopic & scotopic conditions
I	29	N	N	Y	none	none
II	1	Y	N	Y	temporal crescent moon of hyperFAF OU	OS borderline rod response but generally appropriate, cones abnormal centrally and paracentrally OU
II	2	Y	N	Y	hypoFAF from laser scars to HST OU	none

Table 2. (*Continued*)

UWF-FAF Type	ID	Peripapillary Sparing (Y/N)	Fovea Sparing (Y/N)	OS Same? (Y/N)	Other UWF- FAF Findings	ERG Results
II	5	Y	Y	N—not fovea sparing OS	posterior pole hypeFAF OU	grossly normal rod, slightly decreased cone with abnormalities centrally
II	8	Y	Y	Y	none	none
II	11	Y	N	Y	peripheral nasal and temporal mottled FAF OU	rods normal slightly decrease cone isolated amplitudes
II	15	Y	N	Y	hyperFAF at edge of flecks OU	none
II	16	Y	N	Y	hyperFAF at edge of flecks OU	none
IIIa	3	Y	N	Y	hyperFAF at edge of flecks OU	none
IIIa	6	Y	Y	N—not fovea sparing OS	none	none
IIIa	19	Y	N	Y	hyperFAF at edge of flecks OU	none
IIIa	24	Y	N	Y	hyperFAF at edge of flecks OU	none
IIIa/IIIIb	14	Y	N	Y	none	severely depressed across all stimuli, cone responses barely recordable
IIIa/IIIb	27	Y	N	Y	hyperFAF at edge of flecks OU and posterior pole hypeFAF OU	abnormal cone responses, dark-adapted response mildly abnormal
IIIb	7	N	N	N—peripapillary sparing OS	hyperFAF at edge of flecks OU	none
IIIb	18	Y	Y	Y	hyperFAF at edge of flecks OU	none
IIIb	22	Y	N	Y	none	abnormal across all stimuli, cone-rod pattern of loss, mfERG abnormal at all locations centrally
IIIb	23	Y	N	Y	hyperFAF at edge of flecks OU	none
IIIb	26	N	N	Y	hyperFAF at edge of flecks OU	severe dysfunction of cone and rod systems
IIIb	28	Y	N	Y	none	none
IIIc	20	Y	N	Y	posterior pole hypeFAF OU	none
IIIc	21	N	N	Y	hyperFAF at edge of flecks OU	none
IIIc	25	N	N	Y	hyperFAF at edge of flecks OU	none

CF, counting fingers; HM, hand motion; HST, horseshoe retinal tear; hyperFAF, hyperautofluoresence; hypoFAF, hypoautofluoresence; N, no; OD, right eye; OS, left eye; OU, both eyes; VA, visual acuity; Y, yes.

decreased hyper- and hypoautofluoresence (Figure 9). Additionally, in 17.2% of eyes (10/58) on UWF-FAF, there appeared to be peripheral flecks and atrophy that respected an inferior demarcation (Figure 10) line thought to be related to closure of the optic fissure,[35] or watershed zone, for choroidal vasculature, with

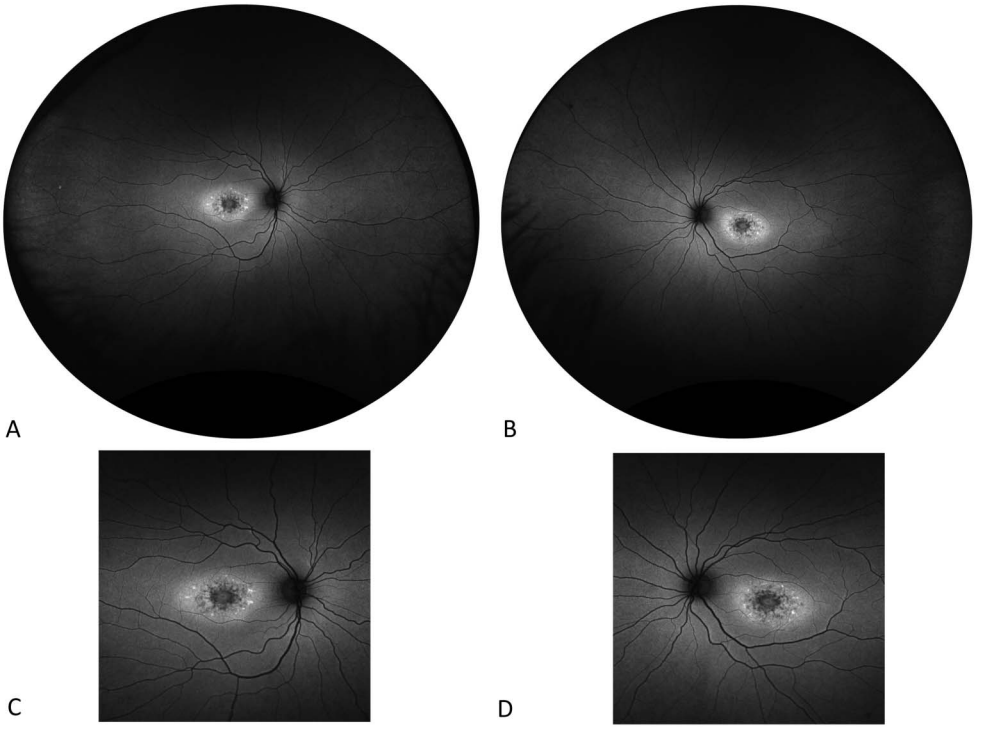

Fig. 1. Type I UWF-FAF pattern in Stargardt disease. Type I pattern with FAF changes confined to the posterior pole (<55° field of view, **A** and **B**). The Optos is also capable of providing high-resolution images of the posterior pole (**C** and **D**) to evaluate the macula in greater detail. These magnified images also depict the typical field of view of current non-widefield FAF systems.

STGD-related abnormalities more prominent on the temporal aspect of this demarcation line.

Genotype results for this cohort are summarized in Table 2. Eight patients had three abnormal ABCA4 variants detected. Four patients had only one disease-causing mutation identified by the genetic testing methods performed. Two patients had homozygous mutations. Three patients were siblings (Subjects 23, 24, 25). The most common genes identified in this study included: c.2588G>C (6/29, 20.7%), c.5882G>A (5/29, 17.2%), c.4222C>T/c.4918C>T (3/29, 10.3%), c.2041C>T (2/26, 6.9%), c.5917delG (2/29, 6.9%), c5714+5G>A (2/29, 6.9%), c.1622T>C (2/29, 6.9%), c.3113C>T (2/29, 6.9%), c.71G>A (2/29, 6.9%), and c.5461-10T>C (2/29, 6.9%).

Electroretinography (full field, and some cases with multifocal testing as noted, Table 2) was performed and available for review in 41.4% of patients (12/29). Severely reduced ERG was noted in three cases, and this was associated with UWF-FAF classification of Type III in all cases. In the remaining nine cases with only mild reduction of amplitudes on scotopic and photopic ERG, UWF-FAF classification was either Type I or Type II.

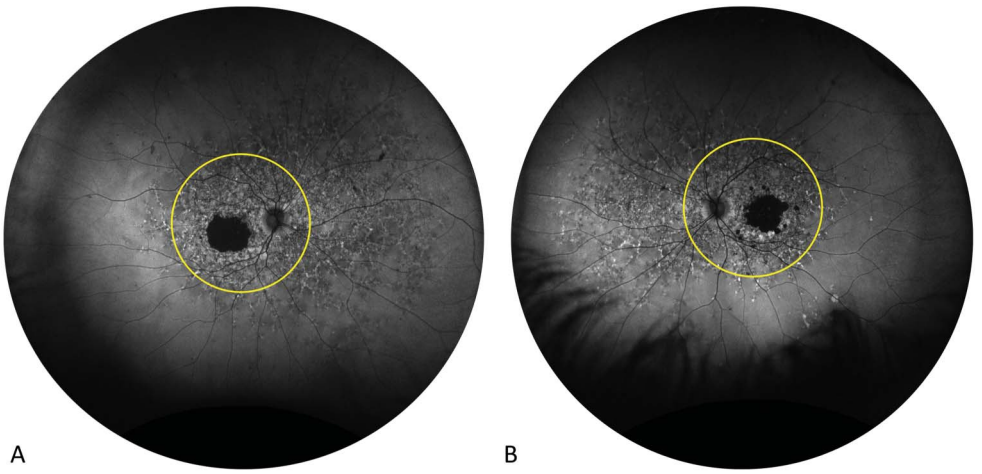

Fig. 2. Type II UWF-FAF pattern in Stargardt disease. Type II pattern displays central atrophy with increased hyper- and hypoautofluorescent changes secondary to the flecks extending to the equator (**A** and **B**). Note there is no significant periphery atrophy. The FAF changes secondary to flecks may also extend anterior to the equator in this Type II classification.

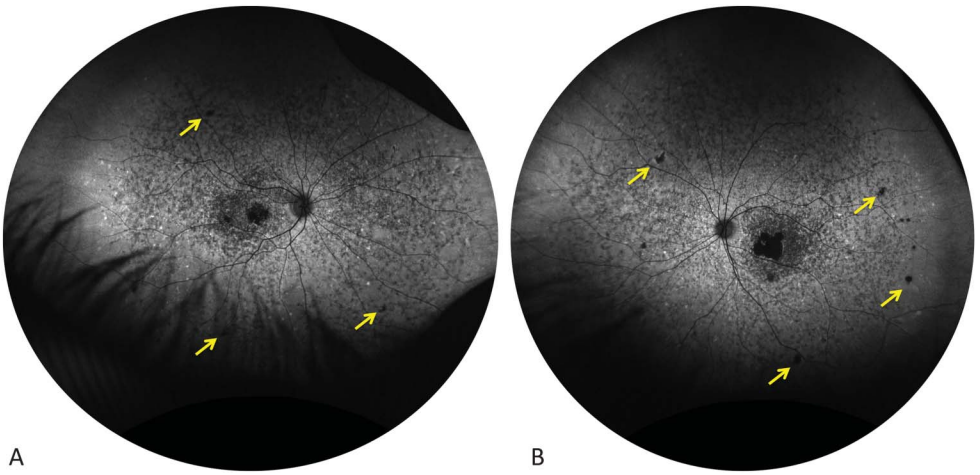

Fig. 3. Type IIIa UWF-FAF pattern in Stargardt disease. Type IIIa pattern displays central and mild peripheral atrophy most often in a punctate, circular pattern (**A** and **B**, yellow arrows). There are most often also mottled areas of increased hyper- and hypoautofluorescent changes secondary to flecks extending to the equator and/or anterior to the equator.

Discussion

This is the initial report correlating UWF-FAF patterns as a feature of STGD phenotype with ABCA4 confirmed genotypes. Images were classified into three types: Type I with findings restricted to the posterior pole with no peripheral FAF changes; Type II with central atrophy only, and with peripheral flecks and associated FAF changes; and Type III with macular atrophy, peripheral FAF changes secondary to flecks, and varying degrees of peripheral atrophy. The presence of peripheral findings was defined as abnormalities outside the 55° field of view of current nonwidefield FAF systems.

Ultrawidefield imaging is an emerging technology that has been instrumental in the diagnosis, management and treatment of many vitreal-retinal conditions including diabetic retinopathy,[36] retinal vascular occlusions,[37,38] sickle cell retinopathy,[39] ocular oncology,[40] retinal detachment,[41] age-related macular degeneration,[42] retinopathy of prematurity[43] and uveitis.[44] Regarding retinal degenerations, recent studies have been published on retinitis pigmentosa, cone/cone-rod dystrophy, and choroidal dystrophies.[32,45–47] One of these studies suggested that objective UWF-FAF findings could be used to estimate visual field function in retinitis pigmentosa.[45] Furthermore, the use of the term "Stargardt *macular* dystrophy" may be used to describe the early phenotype of the disease, however, multiple studies have suggested that STGD has generalized retinal dysfunction as measured by ERG[10] and other ancillary testing. This study also confirms that the peripheral retina is a region that is significantly affected in STGD, and as such, UWF-FAF may be an important imaging modality to assist in the monitoring of STGD patients. Our data suggests that more extensive UWF-FAF patterns, such as the Type III pattern as defined in this study, are expected to be associated with more severe panretinal ERG dysfunction. Additional studies are needed to correlate specific UWF-FAF findings and ERG results, particularly with quantitative UWF-FAF.[48–50] Likewise, in future trials of stem cell or gene therapy for STGD,[51,52] particularly with subretinal delivery, UWF-FAF may be an important imaging

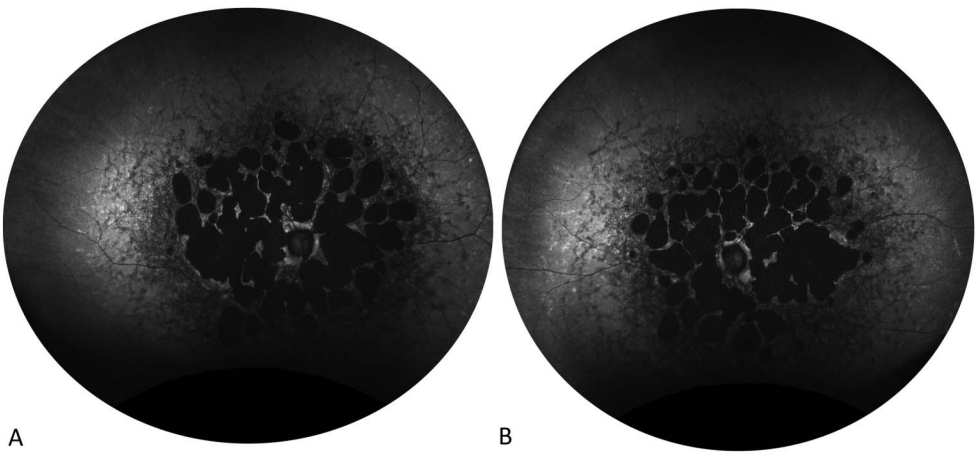

Fig. 4. Type IIIb UWF-FAF pattern in Stargardt disease. Type IIIb pattern displays central and significant peripheral atrophy to the equator but not anterior to the equator (**A** and **B**). There may also be mottled areas of increased hyper- and hypoautofluorescent changes secondary to flecks extending to the equator and/or anterior to the equator.

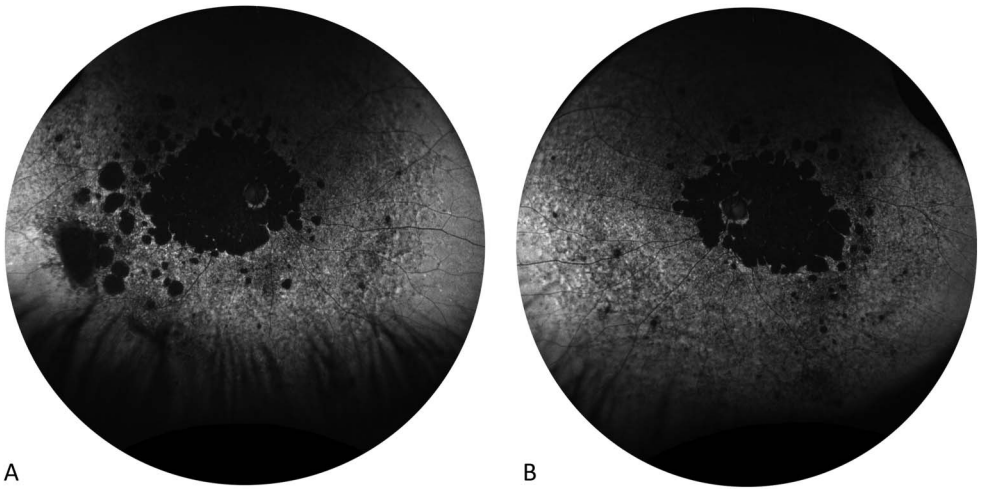

Fig. 5. Type IIIa/IIIb UWF-FAF pattern in Stargardt disease. Type IIIa/IIIb pattern shows not only central and significant peripheral atrophy to the equator but also scattered punctate atrophy anterior to the equator (**A** and **B**). There is no confluent, severe atrophy extending beyond the equator.

modality which may aid in the selection of the optimal location for subretinal delivery of therapeutic agents, based on the presence or absence of FAF abnormalities. Furthermore, identification of transition zones between retina affected by the disorder and less diseased areas (Figure 7) may also be important for disease monitoring, and evaluation of safety and efficacy of novel treatments. Ultrawidefield fundus autofluorescence will be necessary to monitor these transition areas for disease progression if they are located in this peripheral region outside the usual scanning field of traditional imaging systems.

Fundus autofluoresence has been examined extensively in multiple studies of STGD. Despite the widely held belief that lipofuscin accumulation drives RPE cell death in STGD, controversy exists, with reports indicating that the predictive value of hyperautofluoresent lesions to develop into areas of future atrophy

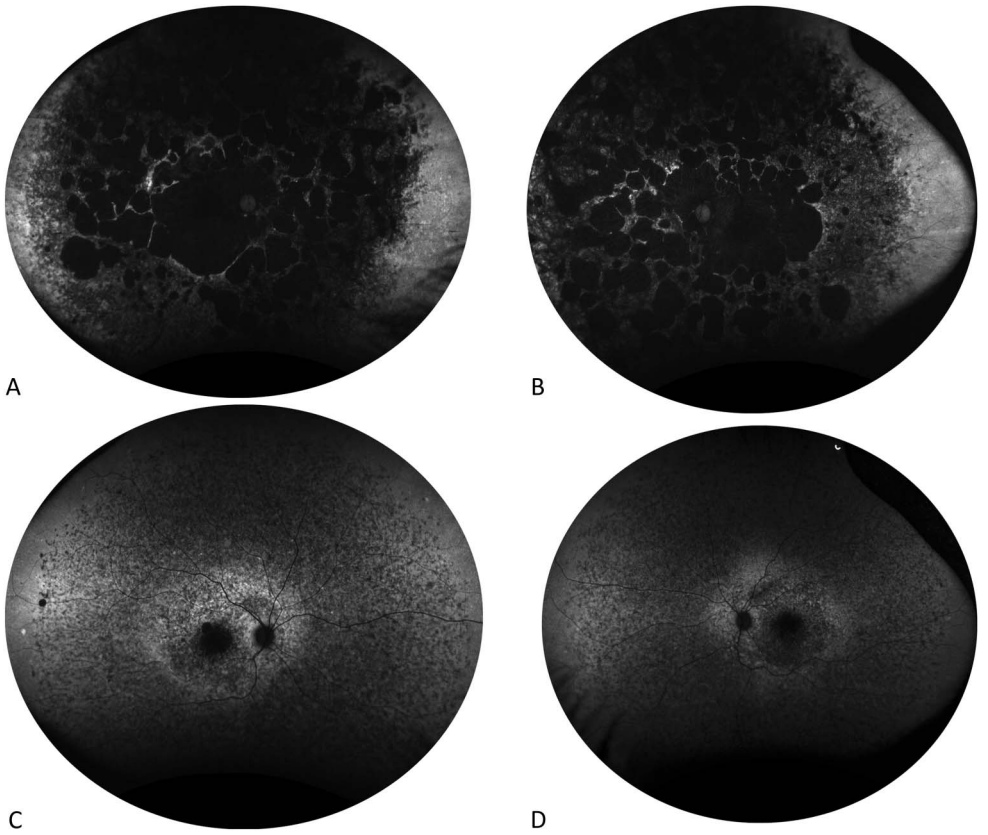

Fig. 6. Type IIIc UWF-FAF pattern in Stargardt disease. Type IIIc pattern displays severe central and peripheral atrophy extending beyond the equator (**A** and **B**). There may be interspersed mottled areas of increased hyper- and hypoautofluorescent changes secondary to flecks extending to the far periphery. Another pattern of severe atrophy on UWF-FAF that extends anterior to the equator (**C** and **D**), which is also Type IIIc, but not in the same large confluent cobblestone pattern as seen above.

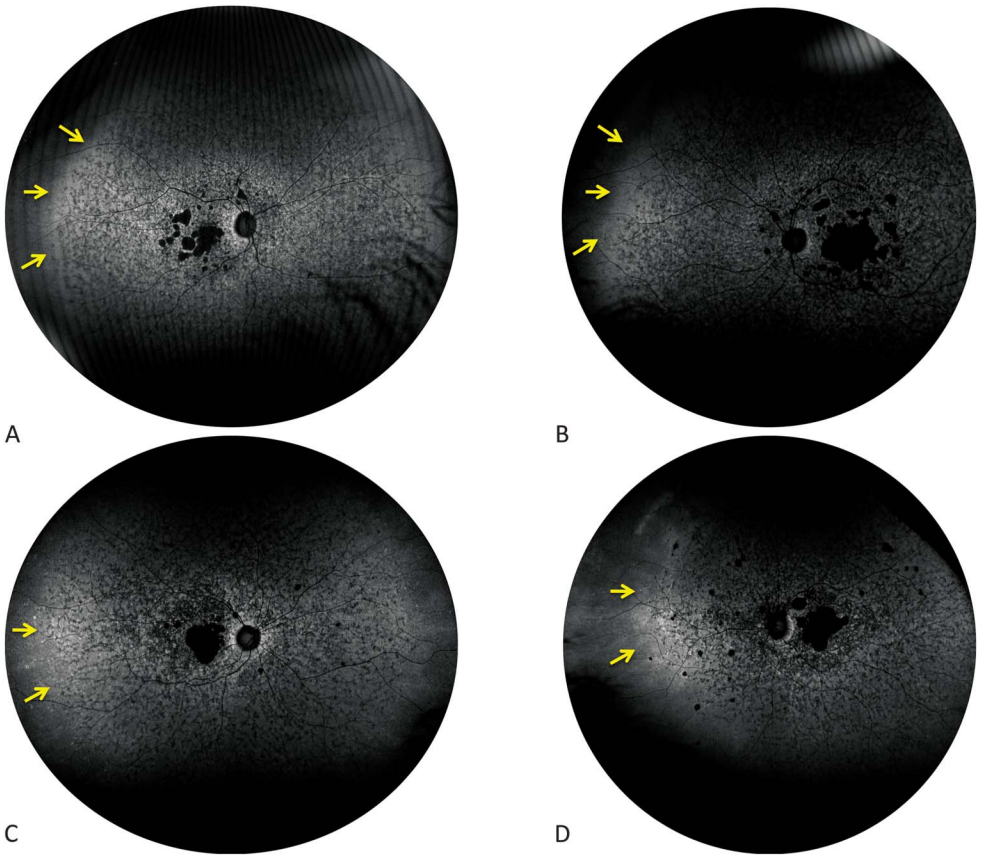

Fig. 7. Increased peripheral hyperautofluoresence. At zones anterior to peripheral flecks and atrophy, there appears to be an area of increased hyperautofluoresence noted in several cases (yellow arrows, **A**–**D**). This may represent a transition zone between posterior diseased retina and less affected anterior retina.

may not always be accurate.[50,53] Groups have reported that FAF in STGD may correlate with biochemical, anatomic, and functional outcomes including visual acuity.[54] Cukras et al have reported that longitudinal FAF imaging over 11 months to 57 months revealed hyperautofluorescent lesions that extended in a centrifugal, radial direction from the fovea, resulting in diminishing FAF with time.[27] They hypothesized that the centrifugal pattern could be attributed to fovea-peripheral gradients of cone photoreceptors and RPE cells in the retina. Other groups have confirmed the predominately centrifugal pattern in STGD[55] indicating that the peripheral fundus is an important site to continue investigating this disorder. Ultrawidefield fundus autofluorescence may provide additional information regarding the dynamic temporal–spatial alterations in STGD by imaging a larger area of the fundus. Of note, the majority of cases in the current report (76%) had peripheral findings that would not have been detected in traditional nonwidefield FAF. Additional longitudinal study of UWF-FAF in STGD may provide insights into the pathogenesis and natural history of STGD.

It is important to note that traditional nonwidefield FAF acquired with devices such as the Heidelberg Spectralis (Heidelberg Engineering, Heidelberg, Germany) use a 488-nm excitation for short-wave FAF, and are also capable of near-infrared FAF with excitation wavelength of 787 nm. In contrast, the Optos UWF-FAF uses a 532-nm excitation wavelength, which may also contribute to the novel findings in this report such as the observed posterior pole increased hyperautofluoresence (Figure 8). Alternatively, given that this particular pattern is not observed in normal patients, one wonders whether this phenomenon in STGD may be related to increased hyperautofluoresence from lipofuscin accumulation, but precedes the clinical detection of flecks on clinical fundus examination or fundus photography. If so, this UWF-FAF pattern may be useful for early disease detection and monitoring. Additional studies are warranted to compare the short-wave UWF-FAF images that may be acquired with the Optos, and systems such as the Staurenghi contact lens that may allow up to 160° of peripheral view and acquisition of widefield near-infrared FAF with properly configured filters.[56] This could be of considerable interest, particularly in cases where the peripheral FAF changes respect an inferior psuedodemarcation line (Figure 10)—this type of UWF-FAF pattern may be even more pronounced with near-infrared wavelength FAF.[55,57]

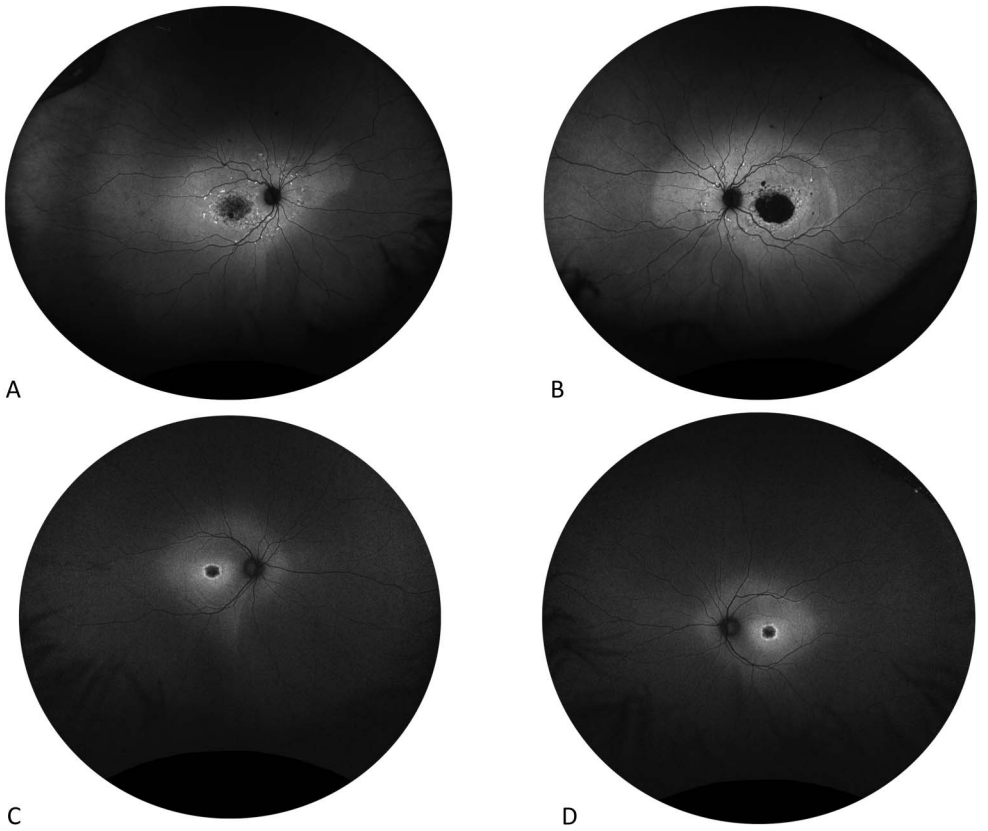

Fig. 8. Posterior pole hyperautofluoresence. Patterns of increased posterior pole hyperautofluoresence are visible in select cases in a circular or oval pattern (**A**–**D**). These may be present with or without peripheral FAF changes secondary to flecks.

A multitude of studies have reported on the genotype/phenotype correlations with ABCA4 Stargardt disease.[4,14,17,23,58] Over 1,000 mutations in the ABCA4 locus have been identified, and there is a high carrier rate of pathologic ABCA4 alleles in the general population. Some ABCA4 mutations may reside in nonexomic sequences, which may not be detected in all sequencing methods. Furthermore, STGD may have a progressive phenotype that changes with time. Together, these facts all make genotype/phenotype correlations challenging in this disorder. One previous study by Sodi et al[30] attempted to compare nonwide-field FAF with different ABCA4 gene mutations in STGD. This study relied on classifying the genotype severity according to two arbitrary groups: splicing/stop/deletion/insertion mutations were classified as severe, and missense mutations were classified as mild.[30] The authors note that their classifications are "partially hypothetical," and we agree given the absence of functional protein data. In comparison with the

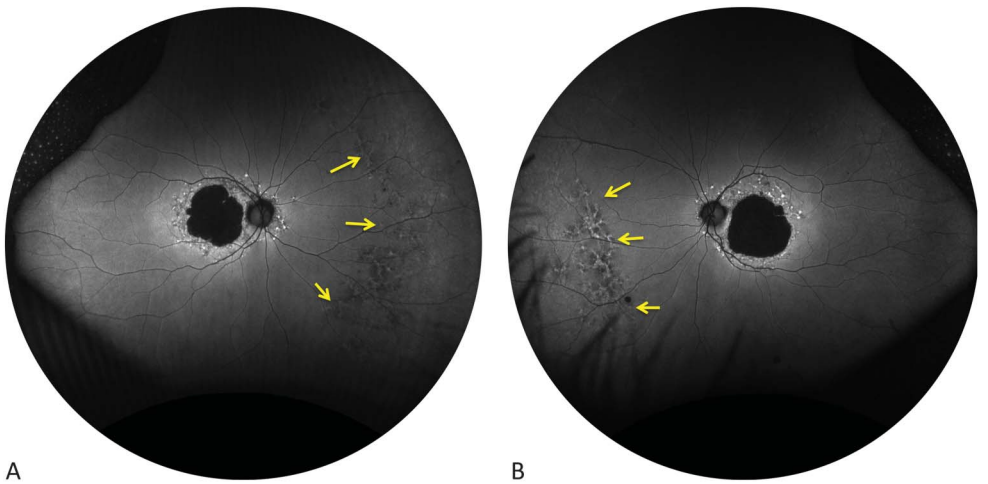

Fig. 9– Peripheral mottled autofluoresence. A single case in a 73-year-old patient (Subject #11) displayed peripheral mottled areas of increased hyper- and hypoautofluoresence (yellow arrows, **A** and **B**).

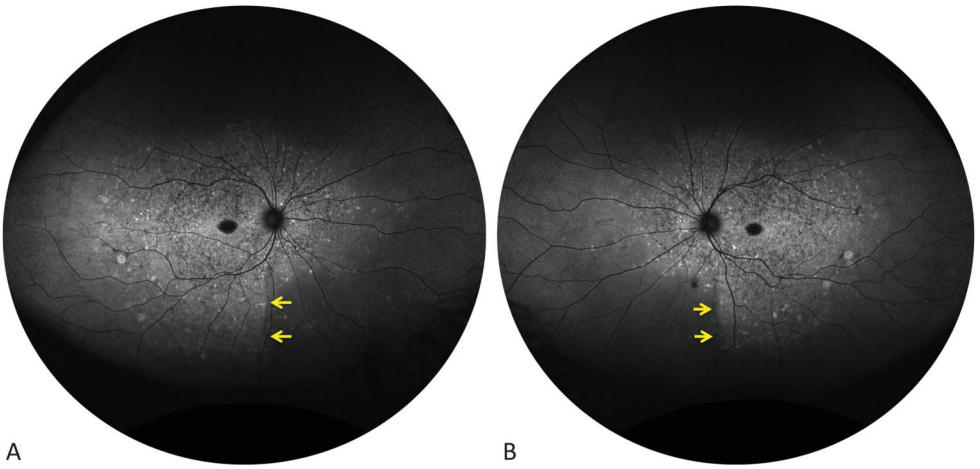

Fig. 10. Peripheral Stargardt disease FAF changes respecting inferior demarcation line. Peripheral UWF-FAF changes secondary to flecks that respect an inferior demarcation line (yellow arrows, **A** and **B**), which can be found in normal subjects and may be anatomically related to closure of the optic fissure. Note the UWF-FAF changes secondary to flecks appear to be more prominent on the temporal aspect of this demarcation line.

genotypes in our study, this Italian group reports the G1961E (c.5882G>A) mutation as mild, and the IVS40+5G>A (c.5714+5G>A) mutation as severe, which were mutations also identified in our study subjects. However, no subjects in either Sodi's cohort or the present study shared the same heterozygous or homozygous genotyping, making meaningful comparisons difficult. Additionally, no individual FAF patterns are reported for each subject, rather the severity of each allele combination (mild/mild vs. mild/severe vs. severe/severe) was used to evaluate the entire group as a whole and attempt to draw conclusions on the FAF patterns.

In the present study, we demonstrate that UWF-FAF supplements the phenotypic profile in a novel way. However, more data is needed to meaningfully segregate peripheral FAF findings into diagnostic or prognostic categories. As such, we believe that the most appropriate approach at this stage is to report the UWF-FAF pattern of each unique genotype along with other demographic characteristics and phenotypic features (e.g., ERG). Though the sample size limits firm genotype/phenotype correlations, the three siblings included in our study (Subjects 23, 24, 25) suggest that the c.4595G>A genotype is associated with more severe atrophy (Type IIIc) than the c.71G>A genotype (Type IIIa or IIIb) on UWF-FAF, given all three subjects also carried the same other allele in trans (c.4222T>C & c.4918C>T). UWF-FAF has the potential to be another metric to stratify the enormous genetic landscape of ABCA4 STGD, however, additional larger prospective studies are needed. Even so, traditional diagnostic modalities such as ERG will continue to be important for monitoring the safety and effectiveness of new therapies for STGD.

Limitations of this study include its retrospective nature with clinical data and imaging collected at only one point in time. Also, other important information such as age of onset of disease was often unavailable and patient accounts may be unreliable. Without longitudinal follow-up, we cannot be certain if these patterns represent progressive stages of STGD or simply a spectrum of disease severity. Future work will address this shortcoming by following patients with STGD over time with serial UWF-FAF imaging. Likewise, not all patients had reliable ERG available for review, which may or may not be another diagnostic modality that can reliably differentiate various subtypes. Furthermore, the majority of patients had exome sequencing as well as examination of ~20 bases of noncoding sequence flanking each exon. However, most of the genetic testing methods used in this study were unable to detect all intronic variants, deletion/insertion variants, or other mutations in other regulatory regions. In the future, as genotype sequencing continues to evolve, it may be of interest to sequence the entire 140 kb ABCA4 locus in all patients to detect additional genetic aberrations, which could provide a more complete picture of the genotype in individual patients.

Conclusion

Fundus autofluoresence is an important diagnostic modality in Stargardt disease. Despite classic early changes in the macula with this heritable disorder, generalized retinal dysfunction is clearly a feature of some, if not all forms of STGD. We report the first series of ultrawidefield imaging in Stargardt disease with confirmed ABCA4 genotypes. Review of UWF-FAF images in this study of STGD patients reveals that abnormalities in the peripheral retina are present in the vast majority of cases and would otherwise be missed on conventional nonwidefield FAF.

Attempts to correlate UWF-FAF phenotypes with ABCA4 genotypes remains a challenge given the

complexity of the ABCA4 locus, and the large number of mutations/variants. The full clinical significance of the UWF-FAF findings in STGD, and in relation to genotype phenotype correlation, will require prospective, longitudinal studies and improved genotyping technologies. As UWF-FAF is increasingly incorporated into patient care, the ability to stage and prognosticate STGD will likely continue to evolve.

Key words: ultrawidefield, ultrawidefield imaging, widefield, imaging, retinal imaging, Stargardt disease/ Stargardt macular dystrophy, retinal degenerations.

References

1. Stargardt K. Über familiare, progressive degeneration in der maculagegend des auges [in German]. Albrecht Von Graefes Arch Klin Exp Ophthalmol 1909;71:534–550.
2. Auricchio A, Trapani I, Allikmets R. Gene therapy of ABCA4-associated diseases. Cold Spring Harb Perspect Med 2015;5:a017301.
3. Rotenstreich Y, Fishman GA, Anderson RJ. Visual acuity loss and clinical observations in a large series of patients with Stargardt disease. Ophthalmology 2003;110:1151–1158.
4. Lambertus S, van Huet RA, Bax NM, et al. Early-onset Stargardt disease: phenotypic and genotypic characteristics. Ophthalmology 2015;122:335–344.
5. Fujinami K, Zernant J, Chana RK, et al. Clinical and molecular characteristics of childhood-onset Stargardt disease. Ophthalmology 2015;122:326–334.
6. Burke TR, Tsang SH, Zernant J, et al. Familial discordance in Stargardt disease. Mol Vis 2012;18:227–233.
7. Michaelides M, Chen LL, Brantley MA Jr, et al. ABCA4 mutations and discordant ABCA4 alleles in patients and siblings with bull's-eye maculopathy. Br J Ophthalmol 2007;91:1650–1655.
8. Gerth C, Andrassi-Darida M, Bock M, et al. Phenotypes of 16 Stargardt macular dystrophy/fundus flavimaculatus patients with known ABCA4 mutations and evaluation of genotype-phenotype correlation. Graefes Arch Clin Exp Ophthalmol 2002;240:628–638.
9. Sunness JS, Steiner JN. Retinal function and loss of autofluorescence in stargardt disease. Retina 2008;28:794–800.
10. Fujinami K, Lois N, Davidson AE, et al. A longitudinal study of Stargardt disease: clinical and electrophysiologic assessment, progression, and genotype correlations. Am J Ophthalmol 2013;155:1075–1088 e1013.
11. Allikmets R, Singh N, Sun H, et al. A photoreceptor cell-specific ATP-binding transporter gene (ABCR) is mutated in recessive Stargardt macular dystrophy. Nat Genet 1997;15: 236–246.
12. Palejwala NV, Gale MJ, Clark RF, et al. Insights into autosomal dominant Stargardt-like macular dystrophy through multimodality diagnostic imaging. Retina 2016;36:119–130.
13. Zhang K, Kniazeva M, Han M, et al. A 5-bp deletion in ELOVL4 is associated with two related forms of autosomal dominant macular dystrophy. Nat Genet 2001;27:89–93.
14. Kjellstrom U. Association between genotype and phenotype in families with mutations in the ABCA4 gene. Mol Vis 2014;20: 89–104.
15. Allikmets R, Shroyer NF, Singh N, et al. Mutation of the Stargardt disease gene (ABCR) in age-related macular degeneration. Science 1997;277:1805–1807.
16. Schutt F, Bergmann M, Holz FG, Kopitz J. Isolation of intact lysosomes from human RPE cells and effects of A2-E on the integrity of the lysosomal and other cellular membranes. Graefes Arch Clin Exp Ophthalmol 2002;240:983–988.
17. Lee W, Xie Y, Zernant J, et al. Complex inheritance of ABCA4 disease: four mutations in a family with multiple macular phenotypes. Hum Genet 2016;135:9–19.
18. Zaneveld J, Siddiqui S, Li H, et al. Comprehensive analysis of patients with Stargardt macular dystrophy reveals new genotype-phenotype correlations and unexpected diagnostic revisions. Genet Med 2015;17:262–270.
19. Zernant J, Xie YA, Ayuso C, et al. Analysis of the ABCA4 genomic locus in Stargardt disease. Hum Mol Genet 2014;23: 6797–6806.
20. Braun TA, Mullins RF, Wagner AH, et al. Non-exomic and synonymous variants in ABCA4 are an important cause of Stargardt disease. Hum Mol Genet 2013;22:5136–5145.
21. Schindler EI, Nylen EL, Ko AC, et al. Deducing the pathogenic contribution of recessive ABCA4 alleles in an outbred population. Hum Mol Genet 2010;19:3693–3701.
22. Heathfield L, Lacerda M, Nossek C, et al. Stargardt disease: towards developing a model to predict phenotype. Eur J Hum Genet 2013;21:1173–1176.
23. Gemenetzi M, Lotery AJ. Phenotype/genotype correlation in a case series of Stargardt's patients identifies novel mutations in the ABCA4 gene. Eye (Lond) 2013;27:1316–1319.
24. Delori FC, Dorey CK, Staurenghi G, et al. In vivo fluorescence of the ocular fundus exhibits retinal pigment epithelium lipofuscin characteristics. Invest Ophthalmol Vis Sci 1995; 36:718–729.
25. Park SP, Siringo FS, Pensec N, et al. Comparison of fundus autofluorescence between fundus camera and confocal scanning laser ophthalmoscope-based systems. Ophthalmic Surg Lasers Imaging Retina 2013;44:536–543.
26. Lois N, Halfyard AS, Bird AC, et al. Fundus autofluorescence in Stargardt macular dystrophy-fundus flavimaculatus. Am J Ophthalmol 2004;138:55–63.
27. Cukras CA, Wong WT, Caruso R, et al. Centrifugal expansion of fundus autofluorescence patterns in Stargardt disease over time. Arch Ophthalmol 2012;130:171–179.
28. Chen B, Tosha C, Gorin MB, Nusinowitz S. Analysis of autofluorescent retinal images and measurement of atrophic lesion growth in Stargardt disease. Exp Eye Res 2010;91:143–152.
29. Fujinami K, Lois N, Mukherjee R, et al. A longitudinal study of Stargardt disease: quantitative assessment of fundus autofluorescence, progression, and genotype correlations. Invest Ophthalmol Vis Sci 2013;54:8181–8190.
30. Sodi A, Bini A, Passerini I, et al. Different patterns of fundus autofluorescence related to ABCA4 gene mutations in Stargardt disease. Ophthalmic Surg Lasers Imaging 2010;41:48–53.
31. Oishi A, Oishi M, Ogino K, et al. Wide-field fundus autofluorescence for retinitis pigmentosa and cone/cone-rod dystrophy. Adv Exp Med Biol 2016;854:307–313.
32. Yuan A, Kaines A, Jain A, et al. Ultra-wide-field and autofluorescence imaging of choroidal dystrophies. Ophthalmic Surg Lasers Imaging 2010;41:e1–e5.
33. Reznicek L, Wasfy T, Stumpf C, et al. Peripheral fundus autofluorescence is increased in age-related macular degeneration. Invest Ophthalmol Vis Sci 2012;53:2193–2198.
34. Witmer MT, Cho M, Favarone G, et al. Ultra-wide-field autofluorescence imaging in non-traumatic rhegmatogenous retinal detachment. Eye (Lond) 2012;26:1209–1216.
35. Duncker T, Lee W, Tsang SH, et al. Distinct characteristics of inferonasal fundus autofluorescence patterns in stargardt

disease and retinitis pigmentosa. Invest Ophthalmol Vis Sci 2013;54:6820–6826.
36. Wessel MM, Aaker GD, Parlitsis G, et al. Ultra-wide-field angiography improves the detection and classification of diabetic retinopathy. Retina 2012;32:785–791.
37. Prasad PS, Oliver SC, Coffee RE, et al. Ultra wide-field angiographic characteristics of branch retinal and hemicentral retinal vein occlusion. Ophthalmology 2010;117:780–784.
38. Tsui I, Kaines A, Havunjian MA, et al. Ischemic index and neovascularization in central retinal vein occlusion. Retina 2011;31:105–110.
39. Cho M, Kiss S. Detection and monitoring of sickle cell retinopathy using ultra wide-field color photography and fluorescein angiography. Retina 2011;31:738–747.
40. Jain A, Shah SP, Tsui I, McCannel TA. The value of Optos Panoramic 200MA imaging for the monitoring of large suspicious choroidal lesions. Semin Ophthalmol 2009;24:43–44.
41. Witmer MT, Cho M, Favarone G, et al. Ultra-wide-field autofluorescence imaging in non-traumatic rhegmatogenous retinal detachment. Eye (Lond) 2012;26:1209–1216.
42. Tan CS, Heussen F, Sadda SR. Peripheral autofluorescence and clinical findings in Neovascular and non-neovascular age-related macular degeneration. Ophthalmology 2013;120:1271–1277.
43. Tsui I, Franco-Cardenas V, Hubschman JP, Schwartz SD. Pediatric retinal conditions imaged by ultra wide field fluorescein angiography. Ophthalmic Surg Lasers Imaging Retina 2013;44:59–67.
44. Campbell JP, Leder HA, Sepah YJ, et al. Wide-field retinal imaging in the management of noninfectious posterior uveitis. Am J Ophthalmol 2012;154:908–911.
45. Oishi A, Ogino K, Makiyama Y, et al. Wide-field fundus autofluorescence imaging of retinitis pigmentosa. Ophthalmology 2013;120:1827–1834.
46. Oishi M, Oishi A, Ogino K, et al. Wide-field fundus autofluorescence abnormalities and visual function in patients with cone and cone-rod dystrophies. Invest Ophthalmol Vis Sci 2014;55:3572–3577.
47. Furutani Y, Ogino K, Oishi A, et al. Intra-familial similarity of wide-field fundus autofluorescence in inherited retinal dystrophy. Adv Exp Med Biol 2016;854:299–305.
48. Kuehlewein L, Hariri AH, Ho A, et al. Comparison of manual and semiautomated fundus autofluorescence analysis of macular atrophy in Stargardt disease phenotype. Retina 2015.
49. Burke TR, Duncker T, Woods RL, et al. Quantitative fundus autofluorescence in recessive Stargardt disease. Invest Ophthalmol Vis Sci 2014;55:2841–2852.
50. Smith RT, Gomes NL, Barile G, et al. Lipofuscin and autofluorescence metrics in progressive STGD. Invest Ophthalmol Vis Sci 2009;50:3907–3914.
51. Sahel JA, Marazova K, Audo I. Clinical characteristics and current therapies for inherited retinal degenerations. Cold Spring Harb Perspect Med 2015;5:a017111.
52. Schwartz SD, Regillo CD, Lam BL, et al. Human embryonic stem cell-derived retinal pigment epithelium in patients with age-related macular degeneration and Stargardt's macular dystrophy: follow-up of two open-label phase 1/2 studies. Lancet 2015;385:509–516.
53. Cukras CA, Wong WT, Caruso R, et al. Fundus autofluorescence patterns in Stargardt disease over time-reply. Arch Ophthalmol 2012;130:1354–1355.
54. Parodi MB, Iacono P, Triolo G, et al. Morpho-functional correlation of fundus autofluorescence in Stargardt disease. Br J Ophthalmol 2015;99:1354–1359.
55. Sparrow JR, Marsiglia M, Allikmets R, et al. Flecks in recessive Stargardt disease: short-wavelength autofluorescence, near-infrared autofluorescence, and optical coherence tomography. Invest Ophthalmol Vis Sci 2015;56:5029–5039.
56. Staurenghi G, Viola F, Mainster MA, et al. Scanning laser ophthalmoscopy and angiography with a wide-field contact lens system. Arch Ophthalmol 2005;123:244–252.
57. Greenstein VC, Schuman AD, Lee W, et al. Near-infrared autofluorescence: its relationship to short-wavelength autofluorescence and optical coherence tomography in recessive Stargardt disease. Invest Ophthalmol Vis Sci 2015;56:3226–3234.
58. Miraldi Utz V, Coussa RG, Marino MJ, et al. Predictors of visual acuity and genotype-phenotype correlates in a cohort of patients with Stargardt disease. Br J Ophthalmol 2014;98:513–518.